A Very Short Hydrogen Bond Provides Only Moderate Stabilization of an Enzyme–Inhibitor Complex of Citrate Synthase†

Ken C. Usher,‡ S. James Remington,*,‡ David P. Martin,§ and Dale G. Drueckhammer*,§

Institute of Molecular Biology and Departments of Chemistry and Physics, University of Oregon, Eugene, Oregon 97403, and Department of Chemistry, Stanford University, Stanford, California 94305

Received March 14, 1994; Revised Manuscript Received May 3, 1994®

ABSTRACT: Two extremely potent inhibitors of citrate synthase, carboxyl and primary amide analogues of acetyl coenzyme A, have been synthesized. The ternary complexes of these inhibitors with oxaloacetate and citrate synthase have been crystallized and their structures analyzed at 1.70- and 1.65-Å resolution, respectively. The inhibitors have dissociation constants in the nanomolar range, with the carboxyl analogue binding more tightly (K_i = 1.6 nM at pH 6.0) than the amide analogue (28 nM), despite the unfavorable requirement for proton uptake by the former. The carboxyl group forms a shorter hydrogen bond with the catalytic Asp 375 (distance <2.4 Å) than does the amide group (distance ≈ 2.5 Å). Particularly with the carboxylate inhibitor, the very short hydrogen bond distances measured suggest a low barrier or short strong hydrogen bond. However, the binding constants differ by only a factor of 20 at pH 6.0, corresponding to an increase in binding energy for the carboxyl analogue on the enzyme of about 2 kcal/mol more than the amide analogue, much less than has been proposed for short strong hydrogen bonds based on gas phase measurements [>20 kcal/mol (Gerlt & Gassman, 1993a,b)]. The inhibitor complexes support proposals that Asp 375 and His 274 work in concert to form an enolized form of acetyl-coenzyme A as the first step in the reaction.

It has long been recognized that enzymes use binding energy as a means of stabilizing high energy transition states and intermediates in order to facilitate catalysis (Jencks, 1975). It has recently been proposed that an unusually large amount of stabilization of high energy enzyme-bound intermediates and/or transition states may be provided by "short strong" or "low barrier" hydrogen bonds (Cleland, 1992; Gerlt & Grassman, 1993a,b). Analysis of hydrogen bond strengths in the gas phase vs bond lengths indicates a drastic increase in bond energy as the bond length becomes less than ~2.45 Å. Normal hydrogen bonds (>2.45 Å in length) have energies of about 7 kcal/mol while hydrogen bonds shorter than this can have energies of 30 kcal/mol and greater in gas phase measurements (Hibbert & Emsley, 1990). These short hydrogen bonds have been termed low barrier hydrogen bonds as there is predicted to be a single potential energy well with no barrier or a low barrier to proton transfer between the accepting and donating atoms (Kreevoy & Liang, 1980). Low barrier hydrogen bonds have been invoked to explain the stabilization of intermediates in the reactions of enzymes catalyzing proton abstraction from carbon acids, acyl transfer reactions, and phosphodiester displacement reactions (Gerlt & Gassman, 1993a,b).

The crystal structures of phosphorus-containing peptide analogues bound to several zinc proteases including thermolysin (Tronrud *et al.*, 1987) and carboxypenicillopepsin (Fraser *et al.*, 1992) have shown 2.3–2.4 Å distances between a phosphonate oxygen of the peptide analogue and a carboxylate oxygen of the enzyme and have been interpreted as evidence of a low barrier hydrogen bond. However, the potential strength of such interactions and the variation of hydrogen bond strength with length in enzyme–ligand complexes have not been demonstrated. In studying analogues of acetyl-CoA[1] as inhibitors of citrate synthase, we have found crystallographic evidence for unusually short hydrogen bonds in enzyme–inhibitor complexes. Comparison of the binding affinity of compounds forming hydrogen bonds of different lengths has permitted some initial analysis of short hydrogen bond strengths in an enzyme–ligand complex.

MATERIALS AND METHODS

Synthesis of Acetyl-CoA Analogues. Acetyl-CoA analogues CMX and AMX (Figure 1) were prepared by previously described methods (Martin & Drueckhammer, 1992) from 4-aminobutyric acid and 4-aminobutyramide. 4-Aminobutyramide was prepared as described previously (Kleeman *et al.*, 1980).

Inhibition Studies of Citrate Synthase with CMX and AMX. Citrate synthase activity was assayed by monitoring the disappearance of absorbance due to the thioester at 233 nm (Srere, 1969). Inhibition constants were determined from Lineweaver–Burk plots of 1/rate versus 1/acetyl-CoA concentration at three concentrations of inhibitor. The enzyme concentrations used were 2 nM at pH 8 and 5 nM at pH 6. The inhibitor concentrations were 40, 80, and 160 nM for CMX at pH 8; 20, 30, and 40 nM for CMX at pH 6; and 450, 900, and 1800 nM for AMX at pH 8. The acetyl-CoA concentrations used were 0.05–0.20 mM at pH 6 and 0.032–0.14 mM at pH 8. 0.5 mM oxaloacetate was used throughout.

X-ray Crystallography of Citrate Synthase: Inhibitor Complexes. CMX and AMX were cocrystallized in ternary

† This work was supported by National Institutes of Health Grant GM45831 (D.G.D.) and National Science Foundation Grant MCB 9118302 (S.J.R.). Acknowledgment is made to the Donors of The Petroleum Research Fund (Grant 25379-G, D.G.D.), administered by the American Chemical Society, for partial support of this research.

* Correspondence regarding crystallography should be addressed to S.J.R., and correspondence regarding synthesis and inhibition studies should be addressed to D.G.D.

‡ University of Oregon.

§ Stanford University.

® Abstract published in *Advance ACS Abstracts*, June 1, 1994.

[1] Abbreviations: CoA, coenzyme A; rms, root mean square; CMC, carboxymethyl coenzyme A; CMX, carboxymethyldethia coenzyme A; AMX, amidocarboxymethyldethia coenzyme A.

0006-2960/94/0433-7753$04.50/0

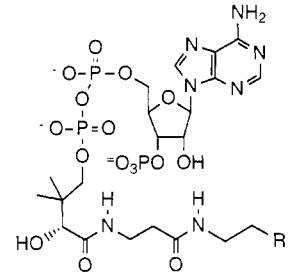

Acetyl CoA, R = $S-\overset{O}{\overset{\|}{C}}-CH_3$

AMX, R = $CH_2-\overset{O}{\overset{\|}{C}}-NH_2$

CMX, R = $CH_2-\overset{O}{\overset{\|}{C}}-O^-$

CMC, R = $S-CH_2-\overset{O}{\overset{\|}{C}}-O^-$

FIGURE 1: Covalent structures of the substrate (acetyl-CoA) and substrate analogues used (carboxylate, CMX and primary amide, AMX) and referred to [carboxymethyl-CoA, CMC (Karpusas *et al.*, 1990)] in this work.

complexes with chicken heart citrate synthase (Sigma) and oxaloacetate, in a "closed conformation" crystal form isomorphous to that observed in ternary complexes containing citrate and CoA, citryl thioether CoA (Remington *et al.*, 1982), and oxaloacetate and carboxymethyl-CoA (Karpusas *et al.*, 1990). The enzyme (0.2 mM in 0.5 M citrate, pH 6.0) was mixed with oxaloacetate (5 mM) and inhibitor (0.5 mM) before crystallization by vapor diffusion against sodium citrate, 0.9–1.1 M (pH 6.0). The inhibitor was isolated in a mixture with potassium phosphate so that 0.1 M phosphate was also present, but this did not appear to affect crystallization, which produced crystals of dimensions up to 0.5 × 0.4 × 0.2 mm. The space group was $C2$, with cell dimensions a = 104.4 Å, b = 78.5 Å, c = 58.5 Å, and β = 78.9°.

Data were collected using a Xuong-Hamlin multiwire detector and processed using the supplied software (Howard *et al.*, 1985). A model based on the previously solved carboxymethyl-CoA ternary complex (Karpusas *et al.*, 1990), deleting all solvent molecules, the side chains of His 274 and Asp 375, and the terminal seven atoms of the CoA analogue, was used for initial refinement against the AMX data using the TNT program package (Tronrud *et al.*, 1987). After initial refinement had converged, the atoms of the new inhibitor as well as the His 274 and Asp 375 side chains were built in on the basis of the $F_o - F_c$ difference electron density map using the FRODO programs (Jones, 1978), and the solvent molecules from the previous model were added. New water molecules were placed (with initial B values of 30 Å^2) where peaks over 4σ in the $F_o - F_c$ map were found and at least one hydrogen bond to the protein could be formed. Correlated temperature factors were refined to produce a final model with the AMX inhibitor, and water molecules whose B values increased over 65 Å^2 were deleted. A $2F_o - F_c$ electron density map calculated using the AMX coordinates and the CMX diffraction data showed that the same model fit very well to both sets of data, so the refined AMX model was used as a basis for the CMX model, with the sole change that the amide nitrogen atom was renamed to an oxygen atom. This model was then refined to convergence against the CMX diffraction data.

Observed differences between CMX and AMX binding were tested for significance in four ways. First, the two diffraction data sets were scaled together and an $F_{o,AMX} - F_{o,CMX}$ difference electron density map was calculated. The atomic model was used to calculate phases for the map, and for this purpose the refined AMX model, excluding the His 274 and Asp 375 side chains and the terminal four atoms of the inhibitor, was used. The map was calculated to 2.0-Å resolution in order to obtain a high percentage of matching reflections. Matching data were obtained for 73% of all possible reflections between 25 and 2.0 Å. Second, the groups involved in the inhibitor to Asp 375 hydrogen bonds in each model were moved using FRODO, artificially shortening or lengthening the distance between them, and were then subjected to more refinement. Third, in order to estimate the coordinate errors of the models, the JIGGLE command in the TNT package of programs (Tronrud *et al.*, 1987) was used to introduce random coordinate errors into all atoms of the two refined structures. Atoms were moved in random directions with normally distributed shift vector lengths, such that the rms deviation in atomic positions from the original was 0.5 Å, with no correlation between movements of neighboring atoms. Five different randomized versions of each model were created, with an average R factor against the crystallographic data of 37%. These were then submitted to 40 rounds of TNT refinement each, after which the refinement had converged, and the resulting models were compared. Any bias introduced in final coordinate positions from details of the choice of initial model is eliminated by this procedure. Fourth, duplicate diffraction data for both AMX and CMX were collected and processed using an R-Axis image plate system and software from Molecular Structures Corporation, and the models were rerefined against these new data.

RESULTS

The acetyl-CoA carboxylate (CMX) and amide (AMX) analogues were studied as inhibitors of the enzyme citrate synthase, which catalyzes the reaction shown in Figure 2. Results are shown in Table 1. CMX was found to be a potent inhibitor of citrate synthase with a K_i 1000-fold lower than the K_m for acetyl-CoA at pH 8.0 and slightly lower than the K_i reported previously (Kurz *et al.*, 1992a) for carboxymethyl-coenzyme A (CMC). AMX was also found to be a potent inhibitor, only slightly weaker than the CMX inhibitor. The K_i for CMX was found to decrease substantially at lower pH, reaching a value of about 1.6 nM at pH 6.0. The K_i for AMX did not change significantly between pH 8.0 and 6.0. Accurate determinations of the K_i for CMX became difficult at low pH, as the K_i became very small. However, the magnitude of decrease in K_i with decreasing pH is consistent with that reported previously (Kurz *et al.*, 1992a) for CMC binding to citrate synthase, as determined using circular dichroism measurements. Errors in the K_i value are certainly less than a factor of 2, which translates to errors in energetics of less than 0.5 kcal/mol. K_i measurements below pH 6.0 were not possible due to a decrease in enzyme activity and stability.

The crystal structures of the ternary complexes of citrate synthase and oxaloacetate with the CMX and AMX inhibitors have been solved (Table 2). The structure with CMX bound shows that it binds as expected for the enol or enolate form of acetyl-CoA, interacting with His 274 and Asp 375 (Figure 3a). Of special note, the carboxylate oxygen of CMX and the carboxylate oxygen of Asp 375 are only 2.38 Å apart. AMX

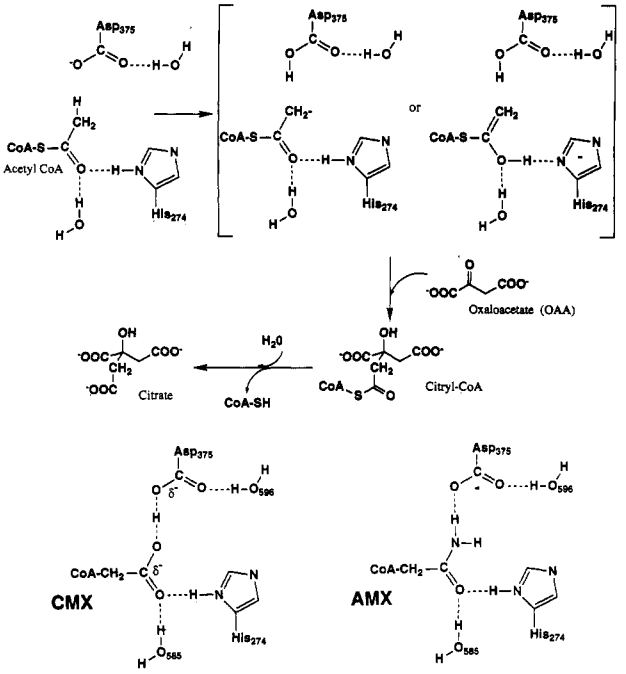

FIGURE 2: (a, top) Proposed reaction mechanism of citrate synthase for the reaction of oxaloacetate and acetyl-CoA to form citrate and CoA (Karpusas *et al.*, 1990; Alter *et al.*, 1990; Kurz *et al.*, 1992a). The charge state of His 274 is shown as being initially neutral, in agreement with the crystal structure where NE1 appears to be a hydrogen bond acceptor, but this is not certain. (b, bottom) Hydrogen-bonding patterns of CMX and AMX inhibitors, showing a similar but not identical pattern to that seen in the proposed mechanism.

Table 1: Inhibition of Citrate Synthase by Acetyl-CoA Analogues

compound	K_i (or K_m) (M)
acetyl-CoA	1.6×10^{-5} (K_m)
CMX (pH 8.0)	1.6×10^{-8}
CMX (pH 6.0)	1.6×10^{-9}
AMX (pH 8.0)	2.8×10^{-8}
CMC (pH 8.0)	4.0×10^{-8}

binds similarly, except that a hydrogen bond distance of about 2.49 Å is observed (Figure 3b). This hydrogen bond cannot occur in the proposed enzyme mechanism, since acetyl-CoA has a methyl group in the equivalent position, from which Asp 375 would abstract a proton in order to allow enolization (Figure 2a,b). Atoms in the active site, including His 274, His 320, Asp 375, the end of the AMX or CMX inhibitor, oxaloacetate, and several tightly bound water molecules, are all very well localized, with temperature factors in the range from 3 to 16 Å^2 (Table 3). Coordinates for these structures have been deposited in the Protein Data Bank, with assigned file names 1CSH (AMX) and 1CSI (CMX).

Both structures are very similar to the one previously reported for CMC and oxaloacetate (Karpusas *et al.*, 1990) at 1.9-Å resolution. The principal difference between the structures of the closely related CMC and CMX inhibitors is the orientation of the terminal carboxyl groups. The CMC inhibitor bulges out somewhat to accommodate the additional sulfur atom in the chain (Figure 4), so that the terminal carboxyl makes a hydrogen bond of poor geometry with the carboxyl of Asp 375, with the unfavorable arrangement that the planes of the two groups are almost perpendicular. In CMX the chain is shorter, with the same number of non-hydrogen atoms as are found in acetyl-CoA, and the two carboxylates are nearly coplanar, resulting in much better hydrogen bond geometry. Corresponding with the improved

Table 2: Diffraction Data and Atomic Model Statistics

	data set	
	AMX	CMX
Refinement Statistics		
no. of crystals	1	2
observations	73408	110637
unique reflections	43148	38694
resolution (Å)	1.65	1.70
completeness (%)[a] (overall)	77	75
25–2.7 Å (%)	93	99
2.7–2.0 Å (%)	69	87
2.0–1.7 Å (%)	73 (1.65 Å)	49
R_{merge} (%)[b]	3.9	5.6
R factor (%)[c]	16.4	15.6
no. of atoms in model		
protein	3391	3391
ligands	60	60
solvent	145	143
Deviations from Ideality (rms)		
bond lengths (Å)	0.013	0.014
bond angles (deg)	3.0	2.7
bad contacts (Å)	0.021	0.023
B correlations (Å^2)	5.4	5.3

[a] Completeness is the ratio in percent of observed to theoretically possible reflections. [b] R_{merge} gives the average disagreement in percent for repeated measurements of an intensity. [c] R factor is the standard crystallographic reliability factor.

geometry, the distance between the two closest oxygens drops from 2.6 Å in the CMC model to 2.38 Å for CMX.

The high quality of the data collected for the current structures enabled a number of additions and corrections to be made in the starting protein model. The carboxyl-terminal residues 434–437 and surface loops at residue 83 and at residues 292–294, which could not be located in $2F_o - F_c$ electron density maps of the previous (CMC) model, were visible and were added to the model. Forty-six presumed water molecules were added. The amino acid sequence for the chicken enzyme, as deduced from the available pig enzyme sequence and the electron density map, is given in the Supplementary Material.

The $F_{o,AMX} - F_{o,CMX}$ difference map (Figure 5) provides good evidence that the change in the inhibitor–Asp 375 hydrogen bond length, although small, is a statistically significant result of the chemical difference between the two inhibitors. The paired positive and negative peaks next to the oxygens of Asp 375 represent a shift which is accounted for primarily by a rotation about the χ_1 angle of the aspartate side chain. The positive and negative peaks around the atom (amide nitrogen in AMX, carboxyl oxygen in CMX) of the inhibitor closest to Asp 375 show that it also moves. The peaks around Asp 375 are both the same height in the map ($\pm 6\sigma$), while around the inhibitor the peak on the side of the CMX oxygen is much higher (-7.5σ) than the two small peaks ($+4\sigma$) on the side of the AMX amide nitrogen. This may be due to the net loss of one scattering electron in going from oxygen to nitrogen or to an increase in the temperature factor of the nitrogen atom (Table 3). These features near Asp 375 and the CMX oxygen represent the three largest peaks in this map and appear just as one as one would expect from a lengthening of the hydrogen bond between them. No difference peaks larger than 4σ were found in the $F_{o,AMX} - F_{o,CMX}$ map away from the active site. Two other smaller features within the active site indicate small movements of the rings of His 274 and Phe 397. An R_{iso} of 4.7% is obtained after the two data sets are scaled together, which is in the same range as the R_{merge} for either individual data set, further indicating the overall similarity of the two structures.

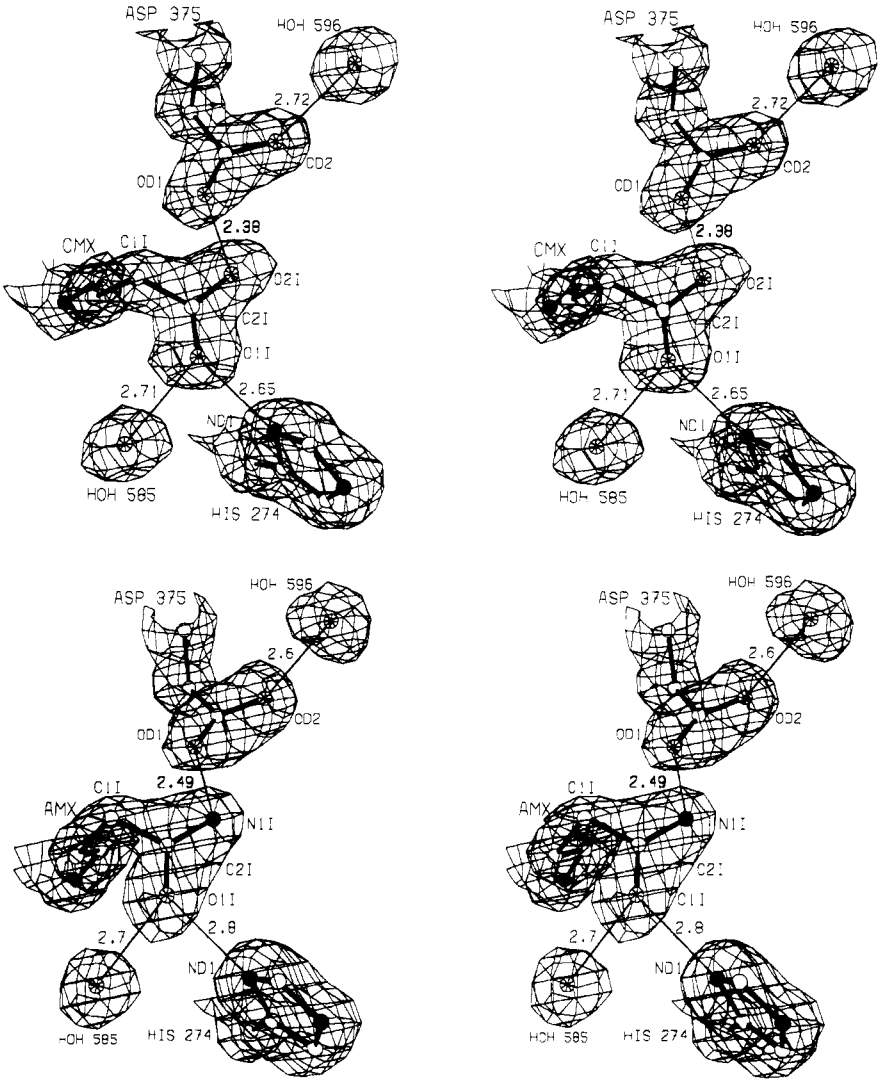

FIGURE 3: Stereoview of the final models and $2F_o - F_c$ electron density maps contoured at 1.5 standard deviations. Carbon atoms are open, oxygen atoms are spoked, and nitrogen atoms are filled. The side chain of Asp 375 and the terminal seven atoms of the inhibitor are shown, as are the other hydrogen-bonding partners of these two groups. Presumed hydrogen bonds are shown by thin bonds, with the O–O or N–O distances marked beside them. (a, top) Ternary complex with CMX (carboxyl analogue), showing the very short hydrogen bond distance between Asp 375 and CMX. (b, bottom) AMX (primary amide analogue), with a somewhat longer hydrogen bond to Asp 375.

Table 3: Statistics from Randomized Models

	model	
	AMX	CMX
no. of models compared	6	6
Asp 375 (OD1)/Inhibitor (O2I/N1I) Hydrogen Bond Length		
mean length (Å)	2.49	2.38
std deviation (Å)	0.02	0.01
Pairwise rms Coordinate Deviations between Models		
Cα atoms (Å)	0.054	0.055
all protein atoms (Å)	0.136	0.136
Selected Temperature Factors (Å^2)		
Asp 375 OD1	16.9	11.3
Asp 375 OD2	13.0	10.3
inhibitor (CMX/AMX)		
C1I	9.0	≤3.0
C2I	9.4	6.3
O1I	9.8	5.1
O2I/N1I	12.1	4.0
His 274 ND1	8.0	5.1
water 585	8.0	≤3.0
all Cα atoms (mean)	14.0	11.3

To assess the accuracy of these distance measurements, the hydrogen bond lengths between Asp 375 and the inhibitor were exaggerated or reduced by manipulating the model, and it was found that refinement returned the atoms to within 0.02 Å of the original positions. The families of refined structures obtained after randomizing and re-refining the positions of the atoms of the two original models also yield an estimate of the error in positioning of the atoms of the model. After refinement, the geometry statistics and *R* factors of the randomized models were equivalent to those of the starting models. Pairwise comparisons between the structures yielded an average of 0.05 Å rms deviation in the positions of all Cα atoms and 0.13-Å deviation for all protein atoms (Table 3), with the increase in the latter likely to be due to inclusion of poorly localized surface atoms. These values are in agreement with coordinate errors estimated by the method of Luzzatti (1952) (not shown), which predicts a mean coordinate error of about 0.15 Å. On the other hand, the hydrogen bond lengths between the inhibitors and Asp 375 are quite invariant, with a standard deviation of 0.01 Å in the CMX structure and 0.02 Å in the AMX structure. This suggestion that the positions of the atoms involved in that interaction are unusually well-determined is borne out by the observation that the temperature factors of these atoms are all very low (Table 3). Bott and Frane (1990) have shown that atoms with low temperature factors have smaller

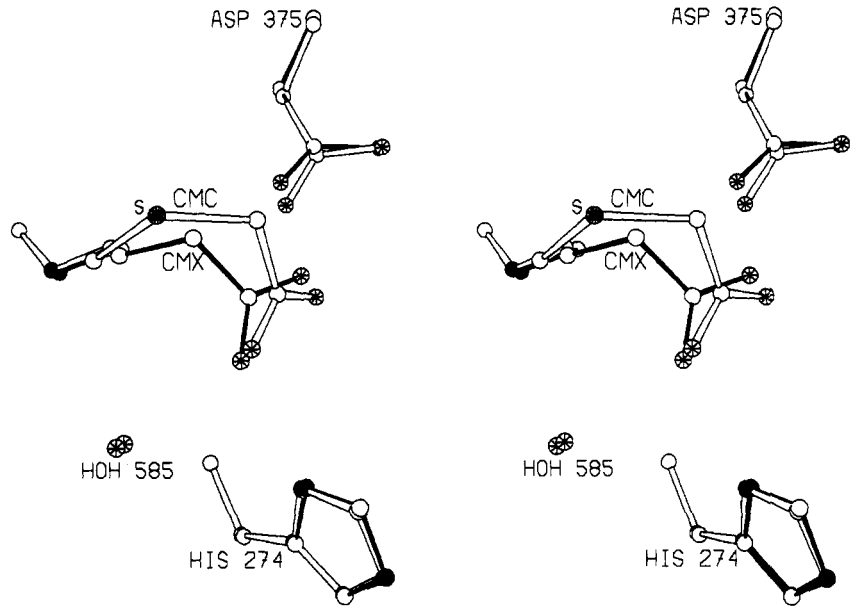

FIGURE 4: Comparison of CMC and CMX carboxyl inhibitors. CMC (open bonds) is made longer by addition of a sulfur atom (labeled by S). Its carboxylate oxygens occupy positions similar to those of CMX (filled bonds), although the geometry of the hydrogen bond made to Asp 375 is changed.

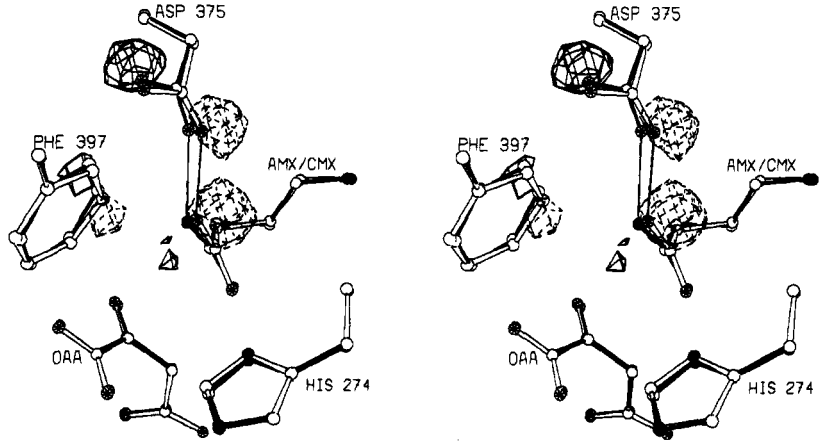

FIGURE 5: $F_{o,AMX} - F_{o,CMX}$ difference map, contoured at −4 standard deviations (dashed density) and +4 standard deviations (solid density), with final refined positions of the AMX (solid bonds) and CMX (open bonds) models superimposed. Bound oxaloacetate (OAA) and the three protein side chains which show small shifts between the two models are included. The critical hydrogen bonds between Asp 375 and each inhibitor are marked with thin bonds.

coordinate deviations between structures than the mean error.

The diffraction data collected using the R-Axis system were of slightly lower resolution (AMX, 39 083 reflections to 1.8 Å, R factor = 14.6%; CMX, 31 936 reflections to 2.0 Å, R factor = 13.3%), due to smaller crystals. However, they produced an $F_{o,AMX} - F_{o,CMX}$ difference map and inhibitor to Asp 375 hydrogen bond distances which were extremely similar to the ones discussed, demonstrating that the structures are not biased by systematic errors of a particular data collection or reduction technique.

DISCUSSION

The proposed mechanism (Karpusas *et al.*, 1990; Alter *et al.*, 1990; Kurz *et al.*, 1992a,b) of citrate synthase is shown in Figure 2a. Asp 375 acts as the base deprotonating the methyl group. The nucleophilic intermediate thus formed condenses with oxaloacetic acid to form citryl-CoA. Citrate synthase subsequently catalyzes the hydrolysis of the thioester bond of the initial product citryl-CoA to form the products CoA and citric acid. The most intriguing question regarding this mechanism is the exact nature and means of stabilization of the nucleophilic intermediate. This is a fundamental question of relevance to all enzymes catalyzing deprotonation of carbon acids. If the intermediate is an enolate, His 274 is expected to provide some stabilization by hydrogen bonding to the enolate oxygen. Alternatively, His 274 may donate a proton to the carbonyl oxygen in concert with methyl deprotonation to form an enol intermediate. The recent short strong hydrogen bond proposal, as applied to this reaction, suggests that the pK_a of the enol form of acetyl-CoA should match the pK_a of neutral His 274 (Gerlt & Gassman, 1993a,b). A short strong or low barrier hydrogen bond may then form between the oxygen of the "enolic" intermediate and the neutral His 274, with the proton being shared equally between the two.

The carboxylic acid (CMX) and primary amide (AMX) analogues of acetyl-CoA are potent inhibitors of citrate synthase, with K_i values much lower than the K_m for acetyl-CoA. The K_i for CMX was found to decrease substantially at lower pH, which is consistent with protonation of the CMX or Asp 375 carboxylate in forming the enzyme–inhibitor complex. The crystal structure of the complex of citrate synthase with CMX (Figure 3a) shows that the inhibitor binds

as expected for the enol or enolate form of acetyl-CoA, interacting with His 274 and Asp 375. In CMX and AMX the sulfur atom of coenzyme A is replaced by a methylene group, so that these nonhydrolyzable inhibitors contain the same number and organization of non-hydrogen atoms as acetyl-CoA, making them the excellent models for acetyl-CoA binding. Both CMX and AMX bind very similarly to carboxymethyl-CoA (Karpusas *et al.*, 1990), an inhibitor which is longer than acetyl-CoA by one methylene group (Figure 4). This similarity of binding confirms that CMC can represent a transition-state analogue despite being larger than the substrate. The binding interactions of AMX and CMX with His 274 and Asp 375 provide further evidence for the concerted role of these residues in enolizing acetyl-CoA, contrary to interpretations which Man *et al.* (1991) have placed on a mutagenesis experiment with *Escherichia coli* citrate synthase, where they have suggested that the equivalent of Asp 375 (Asp 368) is not involved in the enolization reaction.

The carboxylate oxygen of the inhibitor and the carboxylate oxygen of Asp 375 are only 2.38 Å apart, suggesting the presence of a low barrier hydrogen bond between these two oxygen atoms. AMX binds similarly, except that a hydrogen-bonding distance of about 2.49 Å is observed (Figure 3b). This is still substantially shorter than the typical hydrogen bond length but falls above the ≈2.45 Å transition between normal and very strong hydrogen bonds (Hibbert & Emsley, 1990). A very slight difference in hydrogen-bonding distances might be expected if one compares the van der Waals radii of nitrogen (1.55 Å) versus oxygen (1.52 Å) (Hibbert & Emsley, 1990), but this is insufficient to explain the observed difference in the length of the O–O versus N–O hydrogen bonds. Although the $F_{o,AMX} - F_{o,CMX}$ difference map provides convincing evidence for a *difference* in the lengths of these two hydrogen bonds, their absolute values are uncertain as they are limited by the overall coordinate error of the atomic model, estimated to be at least 0.1 Å for structures at 1.7-Å resolution. This will be a limitation on the use of protein crystallography as a tool for investigating the importance of short strong hydrogen bonds in enzyme mechanisms. More work needs to be directed at obtaining a reliable estimate of the coordinate errors for the best defined parts of the atomic models, which are less than the overall error (Bott & Frane, 1990).

On the other hand, it is also not clear how accurately the 2.45-Å "cutoff" differentiating short strong from normal hydrogen bonds is known nor how steep the transition from one case to the other is. It is interesting, if possibly circumstantial, that our measurements of the lengths of these two hydrogen bonds fall on either side of this cutoff. This is what one would expect if in fact one of these is a short strong hydrogen bond, and the other is not. The enzyme appears to make the minimum adjustments necessary to accommodate the two differing interactions.

The much different pK_as (≈10 pK_a units) between the amide hydrogens of AMX and the carboxylate of Asp 375 may also be taken as evidence against a low barrier hydrogen bond with that inhibitor, though the necessity of pK_a matching for low barrier hydrogen bond formation is not absolutely clear, as discussed below. Finally, the temperature factors of the two oxygen partners in the CMX to Asp 375 hydrogen bond (CMX O2I and Asp OD1) are lower than the nitrogen and oxygen (AMX N1I and Asp OD1) in the AMX case (Table 3), consistent with CMX being more tightly bound and better localized than AMX.

The K_i for CMX at pH 8.0 underestimates the binding affinity, as protonation of either the inhibitor or Asp 375 is required for formation of the complex. Studies of the pH dependence on K_i shows that the K_i for CMX decreases with decreasing pH to a value of about 1.6 nM at pH 6.0. This is ≈20-fold lower than the K_i for AMX, corresponding to a difference in binding energy of ~1.8 kcal/mol. While the pK_a of the carboxylate of CMX is likely to be about 4.8 in solution, the pK_a of Asp 375 is expected to be around 6–6.5 on the basis of interpretations of the pH activity profile of the enzyme (Kosicki & Srere 1961; Gerlt *et al.*, 1991). It is thus expected that the K_i measured at pH 6.0 is very near the minimum, with Asp 375 being titrated as the pH is lowered, rather than the carboxylate of CMX. Even if the CMX carboxylate is the one being titrated, lowering the pH to 4.8 would provide at most ~1 kcal/mol of additional stabilization. While CMX and AMX form hydrogen bonds of different lengths to Asp 375 in the enzyme inhibitor complexes, all other interactions between enzyme and inhibitor in these complexes appear identical. To a simple approximation, the observed difference in binding affinity may be attributed to the greater strength of the shorter hydrogen bond, with the assumption that differences in loss of favorable interactions of CMX and AMX with solvent upon binding to the enzyme are not great. The primary amide and carboxylate groups have the potential to make the same number of hydrogen bond interactions with water in solution, with two donor hydrogens in an amide being replaced by two lone pairs of acceptor electrons in a carboxylate group, although differences in net charge and polarity may cause the strength of the resulting interactions to vary somewhat. The complexes of citrate synthase with CMX and AMX thus provide an interesting system for comparing the strengths of hydrogen bonds of different lengths in enzyme–inhibitor complexes.

The assignment of 1.8 kcal/mol greater energy to the shorter hydrogen bond may be viewed as support for the notion that shorter hydrogen bonds are stronger than ordinary hydrogen bonds in enzyme–ligand complexes, as in the gas phase. It is not clear if this 1.8 kcal/mol is significant given the approximations made in the analysis. However, the conclusion can be made that the energy of the short hydrogen bond in this example is quite low compared to the values of 30 kcal/mol and greater reported in the literature for short (<2.45 Å) hydrogen bonds in the gas phase (Hibbert & Emsley, 1990) and the >8 kcal/mol difference between a normal and short hydrogen bond required to explain the deprotonation of carbon acids by the analysis of Gerlt and Gassman (1993a,b).

Short strong or low barrier hydrogen bonds, in which a proton is proposed to be shared equally between two groups, form a charged species in which the charge may be delocalized over several atoms. Thus some component of the interaction will be electrostatic and therefore the strength of the interaction will depend on the local dielectric constant. The effective dielectric constant in proteins varies according to the local environment (Gilson *et al.*, 1985), but estimates for its values have been made ranging from 4, as measured for crystalline polyamides (Baker & Yager, 1942; Gilson *et al.*, 1985), to 40 or 50 on the surface of subtilisin (Russell *et al.*, 1987). Although our results do support the conclusion that very short hydrogen bonds are stronger than normal hydrogen bonds, the interaction energy on the enzyme is less than has been suggested using gas phase measurements where the dielectric constant is 1. This may be partly due to the higher dielectric constant of the surrounding protein medium.

The short hydrogen bond in the complex of CMX with citrate synthase is formed between the more basic *syn* orbital of the carboxylate of Asp 375 and the less basic *anti* orbital of the carboxylate of the inhibitor (Gandour, 1981; Gandour *et al.*, 1990). This suggests that precisely matched pK_as may not be a prerequisite for low barrier hydrogen bond formation, though it is also possible that these pK_as are perturbed sufficiently by the enzyme to be made identical. Low barrier hydrogen bonds between groups with much different pK_as have been observed in the gas phase, between fluoride ion and alcohols (Hibbert & Emsley, 1990). It is possible that the short hydrogen bond in the complex of citrate synthase with CMX is not an optimal one and that stronger low barrier hydrogen bonds might form between groups with better matched pK_as or more appropriate geometry. Certainly more data are needed to definitively analyze the strength of very short hydrogen bonds in enzyme–inhibitor and enzyme–reactive intermediate complexes and the potential role of such hydrogen bonds in stabilization of high energy intermediates and transition states in enzyme-catalyzed reactions.

ADDED IN PROOF

The X-ray structure of citrate synthase complexed with CMC and oxaloacetate has been redetermined using a new data set collected at 1.55-Å resolution. The model has an R factor of 15.8%, and the observed hydrogen bond distance between CMC and Asp 375 has decreased to 2.41 Å. Despite the poorer geometry of the CMC hydrogen bond, this is essentially the same length as is seen with the CMX inhibitor (2.38 Å). The original CMC structure (Karpusas *et al.*, 1990) was solved at 1.9-Å resolution and showed an apparent distance of 2.6 Å. Comparison of the binding affinities of CMC and CMX versus AMX supports the conclusion that the short hydrogen bonds provide little more binding energy than a normal-length hydrogen bond.

SUPPLEMENTARY MATERIAL AVAILABLE

One table listing the changes from the known pig heart citrate synthase sequence deduced for chicken heart citrate synthase from the X-ray structure (3 pages). Ordering information is given on any current masthead page.

REFERENCES

Alter, G. M., Casazza, J. P., Wang, Z., Nemeth, P., Srere, P. A., & Evans, C. T. (1990) *Biochemistry 29*, 7557–7563.

Baker, W. O., & Yager, W. A. (1942) *J. Am. Chem. Soc. 64*, 2171–2177.

Bott, R., & Frane, J. (1990) *Protein Eng. 3*, 649–657.

Cleland, W. W. (1992) *Biochemistry 31*, 317–319.

Fraser, M. E., Strynadka, N. C. J., Bartlett, P. A., Hanson, J. E., & James, M. N. G. (1992) *Biochemistry 31*, 5201–5214.

Gandour, R. D. (1981) *Bioorg. Chem. 10*, 169–176.

Gandour, R. D., Nabulsi, N. A. R., & Fronczek, F. R. (1990) *J. Am. Chem. Soc. 112*, 7816–7817.

Gerlt, J. A., & Gassman, P. G. (1993a) *Biochemistry 32*, 11943–11952.

Gerlt, J. A., & Gassman, P. G. (1993b) *J. Am. Chem. Soc. 115*, 11552–11568.

Gerlt, J. A., Kozarich, J. W., Kenyon, G. L., & Gassman, P. G. (1991) *J. Am. Chem. Soc. 113*, 9667–9669.

Gilson, M. K., Rashin, A., Fine, F., & Honig, B. (1985) *J. Mol. Biol. 183*, 503–516.

Guthrie, J. P., & Kluger, R. (1993) *J. Am. Chem. Soc. 115*, 11569–11572.

Hibbert, F., & Emsley, J. (1990) *Adv. Phys. Org. Chem. 26*, 255–379.

Howard, A. J., Nielsen, C., & Xuong, N. H. (1985) *Methods Enzymol. 114*, 452–471.

Jencks, W. P. (1975) *Adv. Enzymol. Relat. Areas Mol. Biol. 43*, 219–410 and references therein.

Jones, T. A. (1978) *J. Appl. Crystallogr. 11*, 268–272.

Karpusas, M., Branchaud, B., & Remington, S. J. (1990) *Biochemistry 29*, 2213–2219.

Kleeman, A., Leuchtenberger, W., Martens, J., & Weigel, H. (1980) *Angew. Chem., Int. Ed. Engl. 19*, 627.

Kosicki, G. W., & Srere, P. A. (1961) *J. Biol. Chem. 236*, 2560–2565.

Kreevoy, M. M., & Liang, T. M. (1980) *J. Am. Chem. Soc. 102*, 3315–3322.

Kurz, L. C., Shah, S., Crane, B. R., Donald, L. J., Duckworth, H. W., & Drysdale, G. R. (1992a) *Biochemistry 31*, 7899–7907.

Kurz, L. C., Drysdale, G. R., Riley, M. C., Evans, C. T., & Srere, P. A. (1992b) *Biochemistry 31*, 7908–7914.

Luzzatti, V. (1952) *Acta Crystallogr. 5*, 802–810.

Man, W.-J., Li, Y., O'Connor, C. D., & Wilton, D. C. (1991) *Biochem. J. 280*, 521–526.

Martin, D. P., & Drueckhammer, D. G. (1992) *J. Am. Chem. Soc. 114*, 7287–7288.

Remington, S. J., Wiegand, G., & Huber, R. (1982) *J. Mol. Biol. 158*, 111–152.

Russell, A. J., Thomas, P. G., & Fersht, A. R. (1987) *J. Mol. Biol. 193*, 803–813.

Srere, P. A. (1969) *Methods Enzymol. 13*, 3–11.

Tronrud, D. E., Holden, H. M., & Matthews, B. W. (1987) *Science 235*, 571–574.